1953

An investigation of energy levels in V [52] from the V [51] (d,p) V [52] reaction

Schwager, Joseph E.; Cox, Lyle A.

Massachusetts Institute of Technology

AN INVESTIGATION OF ENERGY LEVELS IN V^{52} FROM THE V^{51} (d, p) V^{52} REACTION

JOSEPH E. SCHWAGER
AND
LYLE A. COX

1953

M-34

AN INVESTIGATION OF ENERGY LEVELS IN V^{52} FROM THE $V^{51}(d,p)V^{52}$ REACTION

by

Joseph E. Schwager and Lyle A. Cox

B. S. United States Naval Academy
(1944)

SUBMITTED IN PARTIAL FULFILLMENT

OF THE REQUIREMENTS FOR THE DEGREE OF

MASTER OF SCIENCE

at the

MASSACHUSETTS INSTITUTE OF TECHNOLOGY

June, 1953

Signature of Authors _____

_____

Certified by _____
Thesis Supervisor

_____
Chairman, Departmental Committee on Graduate Students

A C K N O W L E D G M E N T S

We wish to express our appreciation to the entire staff of the High Voltage Laboratory for their unfailing cooperation throughout this project. Needless to say, this thesis would hardly have been possible without their cooperation.

In particular, we are very grateful for the aid of Professor Buechner, who suggested the problem and provided continual supervision and direction during the entire project. His vast experience was invaluable in the solution of many of the particular questions that arose in the course of the over-all problem.

In addition, Dr. Charles K. Bockelman, Dr. Cornelius P. Browne, and Mr. Anthony Sperduto were extremely cooperative and helpful in aiding us in the use of the machine and endoctrinating us into the laboratory procedures.

We should also like to thank Mrs. Mary E. White for her excellent preparation of the manuscript.

AN INVESTIGATION OF ENERGY LEVELS IN V^{52} FROM THE $V^{51}(d,p)V^{52}$ REACTION

by

Joseph E. Schwager and Lyle A. Cox

Submitted to the Physics Department in Partial Fulfillment of the Requirements for the Degree of Master of Science

A B S T R A C T

For about a year, the MIT-ONR Van de Graaff generator has been in operation. It is capable of accelerating charged particles to energies of about 8.5 Mev and of supplying beam currents of about 0.3 Microampere. The generator accelerates the particles vertically downward into a deflecting magnet which acts as a momentum filter and deflects the beam particles through 90 degrees. The particle beam then travels horizontally through a collimating slit system to impinge upon a thin target. The energy spectrum of the product particles emerging at 90 degrees to the incident beam is analyzed by means of an annular magnetic spectrograph which employs 180-degree focusing. The particles are detected by observing the tracks made on nuclear emulsions. The tracks are counted under a microscope; the number of particles is plotted versus diameter of curvature; and from these plots, the energies of the particle groups are computed. The energy of the incident particles is determined by measuring their deflection after they have been elastically scattered from a known target nucleus.

The above equipment was used to investigate energy levels in V^{52} by the $V^{51}(d,p)V^{52}$ reaction. The energy-level system of V^{52} had previously been investigated, mainly by Bartholomew and Kinsey[2] by means of the $V^{51}(n,\gamma)V^{52}$ reaction. Earlier, (d,p) reactions were reported by Davidson[5], Harvey[8], and Abramov[1].

The targets employed in this survey were made by evaporating thin layers of pure vanadium onto Formvar backings. Special hardware and techniques were developed for the target-preparation process which should be of value in evaporating other high-melting point or scarce materials.

The energy spectrum of the product protons was analyzed and proton particle groups corresponding to the ground state and nineteen excited levels in V^{52} were found in the range of excitation energies from zero to about 3.3 Mev. Of these levels, eight were previously unreported.

[illegible] DECAY OF $A_{2g}(^4P)M_{2g}$ EXCITON

by

Joseph E. Dolbecky and Lyle A. Dee

Submitted to the Physics Department in Partial Fulfillment of the
Requirements for the Degree of
Master of Science

A B S T R A C T

For about a year, the following may be briefly summarized has been in operation. It is capable of accelerating charged particles to energies of about 6.5 Bev and of producing beams corresponds of about 0.5 Microampere. The accelerator accelerates the particles vertically downward into a deflecting magnet which acts as a momentum filter and deflects the beam particles through 90 degrees. The particle beam then enters horizontally through a collimating exit system to impinge upon a brick target. The energy spectrum of the product particles emerging at 90 degrees to the incident beam is analyzed by means of an analyzer magnetic spectrograph which contains 120-degree focusing. The particles are detected by observing the tracks made on nuclear emulsions. The tracks are counted using a microscope; the number of particles in plotted versus distance of curvature; and from these plots, the energies of the particles are computed. The energy of the incident particles is determined by measuring their deflection after they have been classically scattered from a known target material.

The above equipment was used to investigate energy levels in Y_2^{89} by the $Y_2^{89}(d,p)Y_2^{90}$ reaction. The energy-level scheme of Y_2^{90} had previously been investigated mainly by Burkhardt and Sloan[2] by means of the $Y_2^{89}(n,\gamma)Y_2^{90}$ reaction. Earlier, (d,p) reactions were reported by Davidson[3], Sherr[4], and Almqvist[5].

The targets employed in this survey were made by evaporating thin layers of pure natural zinc foamed backings. Special backings were and monolayers were developed for the target-preparation procedure which should be of value in evaporating other high-melting point or coarse materials.

The energy spectrum of the emitted protons was analyzed and photographic recording corresponding to the ground state and nineteen excited levels in Y_2^{90} were found in the range of excitation differences from zero to about 3.5 Mev. Of these levels, eight were previously unreported.

These results are tabulated as follows:

Group	Relative Intensity†	Q-Value in Mev	Level Value in Mev
Ground	0.93	5.072 ± 0.008	0
1	0.36	4.941 ± 0.008	0.131 ± 0.011
2	0.07	4.654 ± 0.008	0.418 ± 0.011
3	0.50	4.292 ± 0.008	0.780 ± 0.011
4	0.75	4.238 ± 0.008	0.834 ± 0.011
5	0.21	3.670 ± 0.008	1.402 ± 0.011
6	0.13	3.597 ± 0.008	1.475 ± 0.011*
7	1.00	3.527 ± 0.008	1.545 ± 0.011
8	0.50	3.319 ± 0.008	1.753 ± 0.011*
9	0.18	3.287 ± 0.008	1.785 ± 0.011
10	0.43	2.984 ± 0.008	2.088 ± 0.011
11	0.40	2.765 ± 0.008	2.307 ± 0.011*
12	0.39	2.657 ± 0.008	2.415 ± 0.011
13	0.10	2.614 ± 0.008	2.458 ± 0.011
14	0.22	2.547 ± 0.008	2.525 ± 0.011*
15	0.21	2.224 ± 0.008	2.848 ± 0.011
16	0.21	2.070 ± 0.008	3.002 ± 0.011*
17	0.41	2.021 ± 0.008	3.051 ± 0.011*
18	0.52	1.883 ± 0.008	3.189 ± 0.011*
19	0.29	1.766 ± 0.008	3.306 ± 0.011*

*Previously unreported.

†For E_d = 5.74 Mev

Thesis Supervisor: W. W. Buechner
Associate Professor of Physics.

Group	Relative Intensity†	Q-Value in MeV	Level Value in MeV
Ground	0.93	5.072 ± 0.006	0
1	0.36	4.941 ± 0.008	0.131 ± 0.011
2	0.07	4.894 ± 0.006	0.178 ± 0.011
3	0.50	4.842 ± 0.007	0.230 ± 0.011
4	0.75	4.832 ± 0.008	0.240 ± 0.011
5	0.21	4.4710 ± 0.0028	0.601 ± 0.012
6	0.13	4.307 ± 0.010	0.765 ± 0.012*
7	1.00	4.321 ± 0.004	0.751 ± 0.011
8	0.60	4.129 ± 0.004	0.943 ± 0.011*
9	0.18	4.077 ± 0.009	0.995 ± 0.011
10	0.43	3.984 ± 0.004	1.088 ± 0.011
11	0.80	3.765 ± 0.008	1.307 ± 0.012*
12	0.39	3.657 ± 0.009	1.415 ± 0.011
13	0.34	3.454 ± 0.004	1.618 ± 0.011
14	0.22	3.364 ± 0.004	1.708 ± 0.011*
15	0.21	3.258 ± 0.007	1.814 ± 0.011
16	0.11	3.179 ± 0.006	1.893 ± 0.012*
17	0.12	3.021 ± 0.004	2.051 ± 0.011*
18	0.42	2.819 ± 0.003	2.253 ± 0.012*
19	0.39	2.766 ± 0.008	2.306 ± 0.011*

*Previously unreported.

†For E_γ = 5.714 MeV

Thesis Supervisor: T. A. Buechner
Instructor in Physics

TABLE OF CONTENTS

I. INTRODUCTION

At the present time, a large continuing problem in the field of nuclear physics is the accurate determination of nuclear energy levels. To date, no theory can correlate these levels. Therefore, in general, the collection of accurate nuclear data is continued in the hope that the data will point the way to an adequate theory of nuclear forces.

For several years, the M. I. T. air-insulated Van de Graaff generator with its annular magnetic spectrograph for particles emerging at 90 degrees to the incident beam provided a most productive method of accurate energy-level determination. The spectrograph provided a means of analyzing the energy of the product particle groups to an accuracy of 0.1 percent. The energy of the bombarding particles was well-defined and regulated so that thin targets would yield clearly defined emergent particle energy groups.

However, a major limitation of this air-insulated generator was the maximum beam energy available; about 2 Mev. This low energy limited the field of investigation to fairly light nuclei.

Within the past year the MIT-ONR generator has been placed in operation and has operated at energies in excess of 8 Mev. Professor Buechner encouraged us to make a preliminary investigation of medium- to high-atomic-numbered elements to determine what special problems might be encountered in this untried region. Since

I. INTRODUCTION

time was a limitation in our problem, we confined our study to elements which are largely monoisotopic in nature. We succeeded in making workable targets of tantalum, cesium, and vanadium and did a small amount of preliminary work on each. Our conclusions were that satisfactory energy surveys in this region were possible but much more complicated.

For our contribution, we chose to investigate nuclear levels in vanadium using the (d,p) reaction, because it presented various intriguing technical challenges; furthermore, current literature has shown recent interest in this element. Of the several ways that data for a reaction can be collected, we measured the number of emergent protons at 90 degrees to the incident deuteron beam versus emergent proton energy for various fixed deuteron input energies. With these data, we calculated Q-values and energy levels for V^{52} using a standard mathematical technique.

The investigation of levels in V^{52} proved to be most interesting, challenging, and fruitful. In fact, so many proton groups were found that we were forced to interrupt our survey at an excitation energy of about 3.3 Mev in order to analyze and present our data within the time allotted to us.

II. APPARATUS AND EXPERIMENTAL PROCEDURE

Part A. Equipment

The general procedure followed in the Laboratory in doing a nuclear reaction of this sort is to bombard a target with a deuteron beam of definite energy and to analyze the energy of the protons which emerge at 90 degrees to the incident beam. If the target is sufficiently thin so that the energies of incident deuteron and emerging protons are not greatly "straggled" in passing through the target material, the emerging particles are found to occur in groups of definite energies. These groups correspond to definite levels of excitation in the residual nucleus.

The major equipment used in this problem was the MIT-ONR Van de Graaff generator, a deflecting magnet, a collimating slit system, and the annular magnetic spectrograph. Figure 1 shows the general layout of equipment in the target room.

MIT-ONR Generator. The principles of operation of the Van de Graaff generator are well known. The outstanding characteristics of this accelerator are that it is able to deliver a particle beam of about 4.0- to 8.5-Mev energy and about 0.3-microampere intensity. Figure 2 shows a cutaway of the generator.

Deflecting Magnet. The deflecting magnet (see Figure 1) serves as a momentum filter for the bombarding particles. The

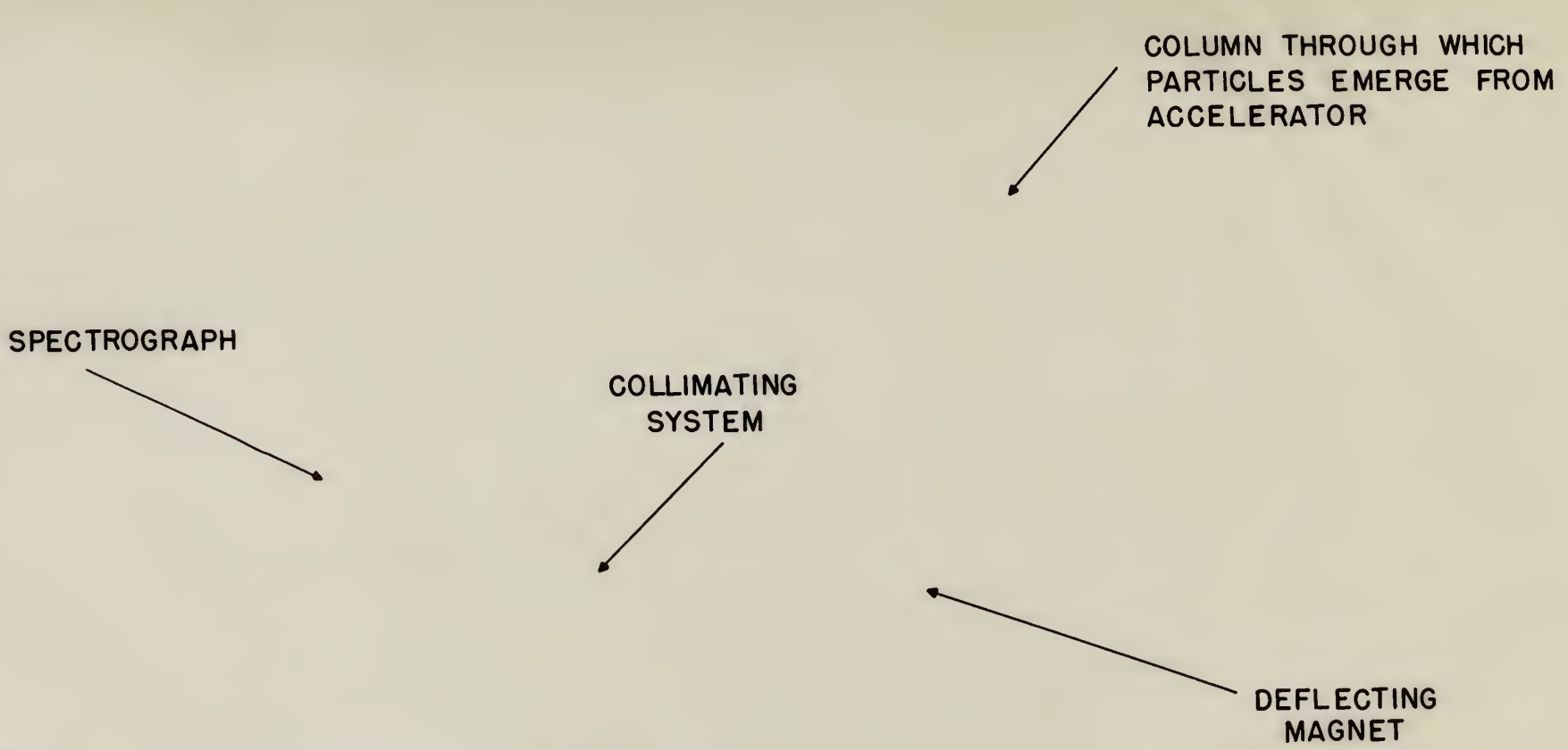
COLUMN THROUGH WHICH
PARTICLES EMERGE FROM
ACCELERATOR
SPECTROGRAPH
COLLIMATING
SYSTEM
DEFLECTING
MAGNET

Figure 1

COLUMN THROUGH WHICH
PARTICLES EMERGE FROM
ACCELERATOR
MAGNET
DEFLECTING
COLLIMATING
SYSTEM
SPECTROMETER

Figure 1

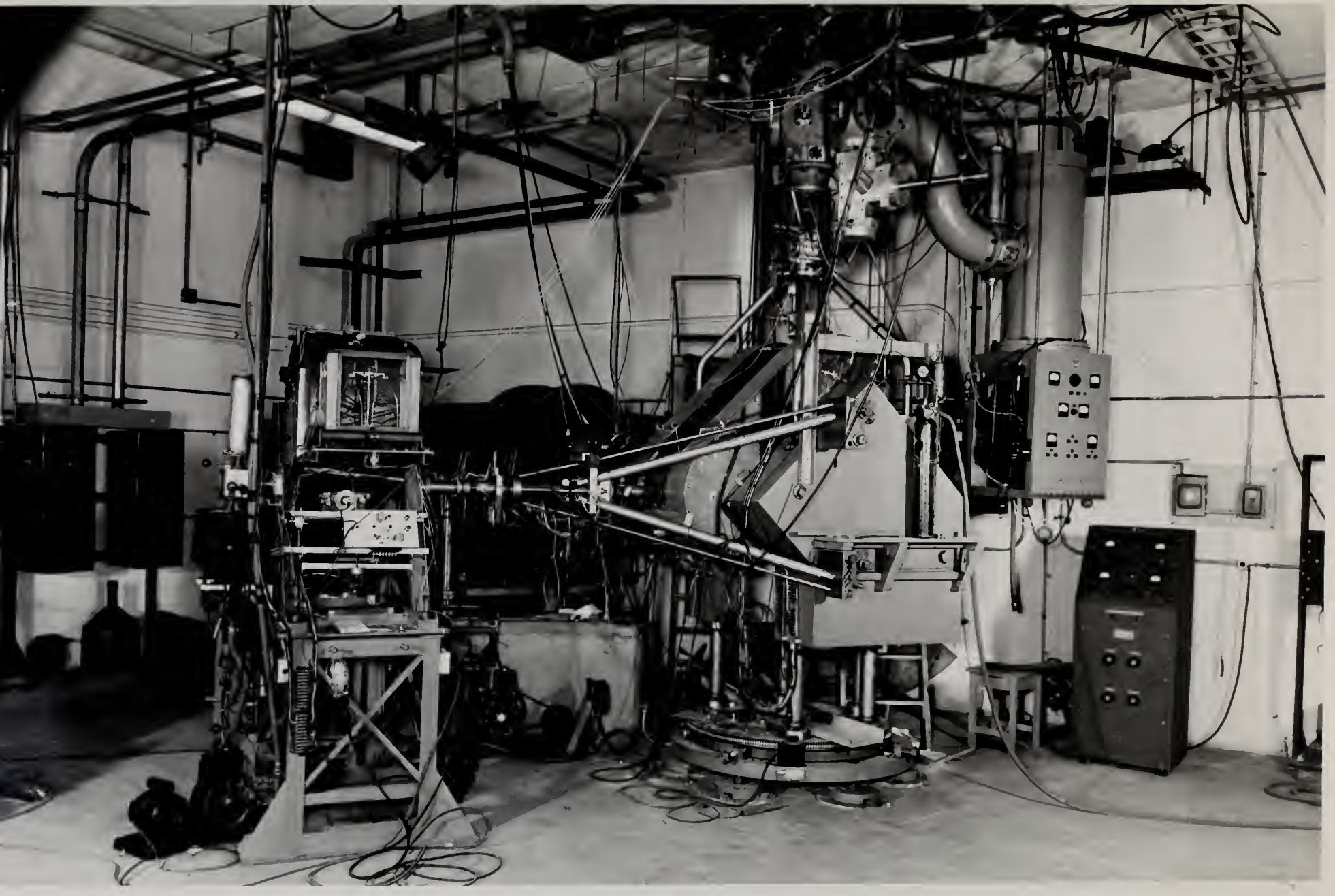

Figure 2. This shows a cutaway of the ONR accelerator

Figure 2. This shows a cutaway of the CMR accelerator

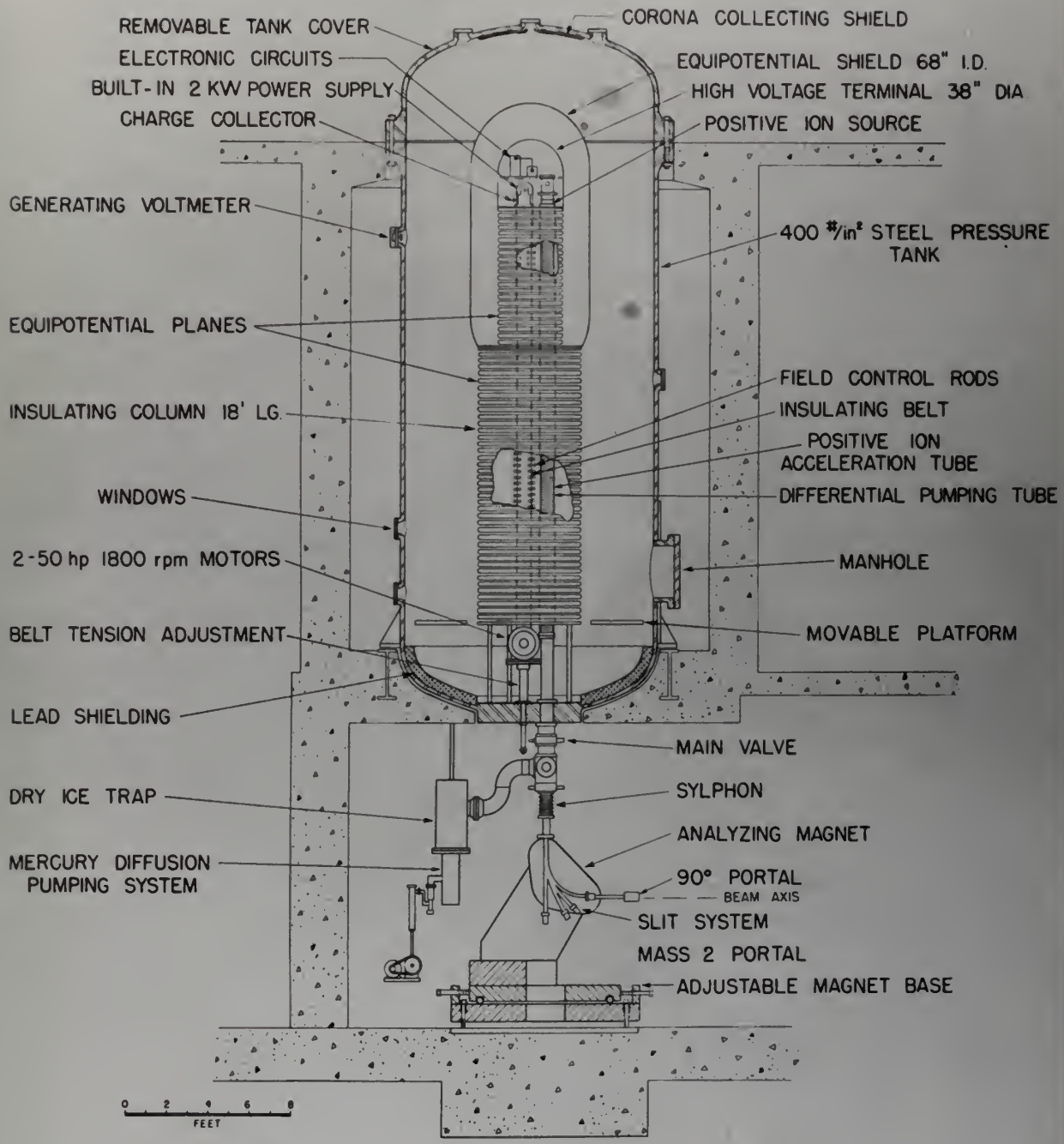

12 MEV POSITIVE ION ACCELERATOR FOR M.I.T.

generator accelerates the particles vertically downward into the deflecting magnet where they are deflected through 90 degrees (when the generator is at the proper voltage) into the slit system. Of course, the mass of the bombarding particle is known so that the momentum filter acts as an energy filter. Thus, the deflecting magnet in conjunction with the slit system serves to define the energy of the beam current.

Slit System. The particle beam after passing through the deflecting magnet, travels about 5 feet horizontally where it passes through an energy-control slit set at about 1 millimeter. It then enters a rectangular slot cut in the first pole piece of the spectrograph where it passes an energy-defining slit, which is a horizontal slit about 1/2 mm wide. The beam then passes through the target located in the pole face gap. The purpose of the slit system is to define the beam, limit its energy spread, and supply a corona-control signal for generator voltage control.

Spectrograph. The spectrograph, see Figures 3 and 4, which has been described in detail by Strait[10], provides a uniform magnetic field whose lines of flux are parallel to the incident beam and extend over an annular region of mean diameter 70 centimeters and about 5 centimeters in width.

Figure 3. A view of the spectrograph, deflecting magnet, and collimating tube.

Figure 3. A view of the spectrograph, deflecting magnet, and collimating tube.

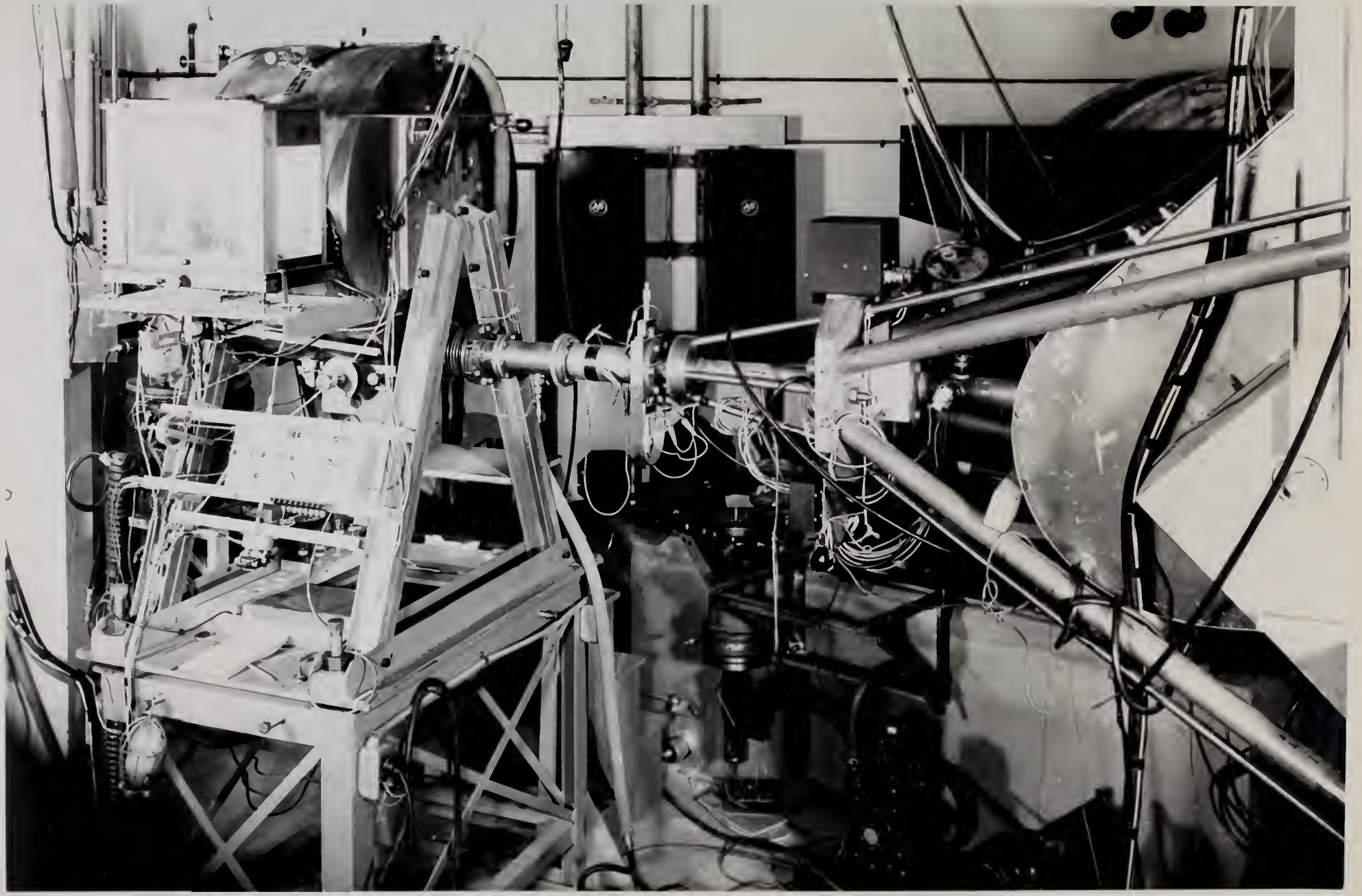

Figure 1. A close-up of the spectrograph where the target chamber at the bottom and the camera box at the top are visible.

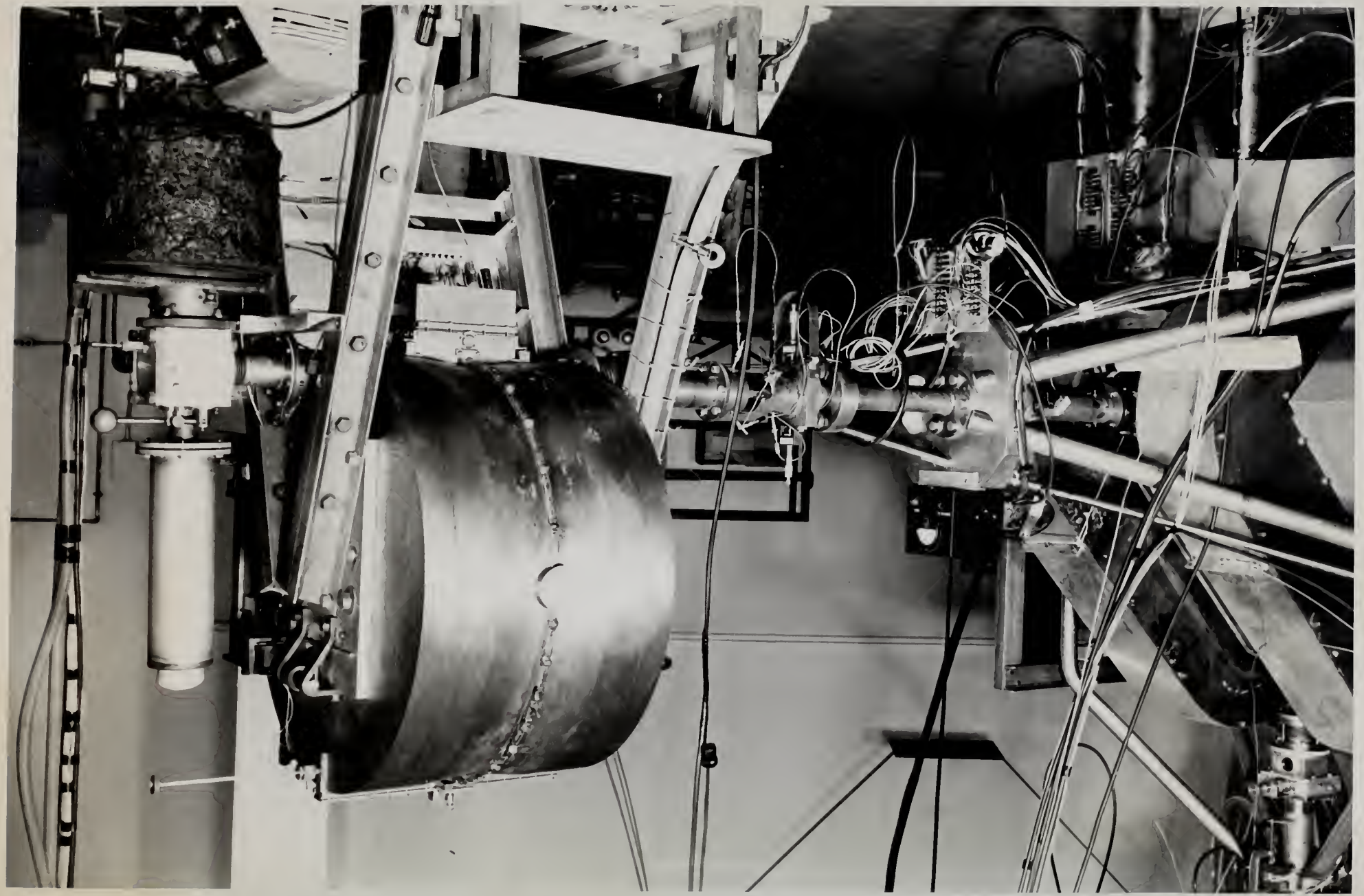

Appended to the spectrograph at the bottom is the target box which houses a rotable wheel, on which seven targets may be mounted radially. Thus, seven targets are available for use without breaking vacuum. The target is so placed that its normal lies about halfway between the direction of the incident beam and that of the charged particle emerging at 90 degrees.

Diametrically opposite to the slot cut to admit the incident beam and target holder, a second slot cut in the pole pieces permits the insertion of the photographic plates used in detecting the charged reaction products. The plates are placed in the field so that the length lies vertically along the diameter of the magnet. Thus, a plate covers a momentum region corresponding to the product of the field and one-half of the effective length of the plate. The Hr covered by a plate is variable depending upon the region; at Hr of about 450 kilogauss-centimeters, the plates covered about 20 kilogauss centimeters. The plates are positioned at about 30 degrees to the plane of the pole pieces. A plateholder, which holds five plates, slides in the camera box and allows for successive exposure of these plates without breaking vacuum.

In conjunction with the camera box is a light and slit system which can cause a sharply defined light beam to shine against the back of the photographic plate when the plate is in the exposure position. This index marks the exact position of the plate in the magnet. Therefore, the distance of a particle group from the

index mark is the amount the diameter of curvature of the group is reduced from the calibrated diameter to the index mark.

Connecting the target chamber with the camera box is the "C" chamber which is a 180-degree annular vacuum box, rectangular in cross section, that is slipped between the pole faces of the magnet. It is through this chamber that the product particles travel from the target to the photographic plates.

The target exposure is measured by an integrating circuit developed by Enge[7]. Most of the particle beam continues through the target, through a rectangular slot in the second pole piece to be collected in a biased Faraday cage, and then integrated.

Auxiliary Equipment and Calibration. The photographic plates were Eastman Kodak NTA emulsions of 60-micron thickness. They were counted by means of a Spencer dark-field, binocular microscope, in which 12X eyepieces were used. The objective lens was 20X or 43X. With 20X objective, the field of view on the photographic plate was one-half millimeter by one-half millimeter. For a given setting along the length of the plate, counts were taken across the readable width of the plate.

The separation of the beam line on the target from the index mark on the photographic plate is measured by means of a polonium alpha-standard. A polonium-coated wire is placed approximately in the target position. The field is set and a plate exposed. A

microscopic measurement of the separation of the beam line from the polonium wire is made by successively positioning a bombarded target and then the polonium wire in the field of the microscope. The separation of the alpha-group from the index, the field setting, and the separation between the wire and the beam position give a measure of the diameter from beam to index.

The magnetic field is adjusted and measured by the nuclear magnetic-moment resonance method. This method consists essentially of measuring the frequency at which quantum jumps of the orientation of the magnetic moments of Li^7 or a proton occur in an aqueous solution of LiCl. The LiCl is contained in a small glass capsule positioned in the center of the pole face gap. A secondary standard is used for frequency measurement. It is "zero beat" daily against one of the broadcast frequency standards of Bureau of Standards station WWV.

Part B. Experimental Procedure

The experimental procedure which was followed was roughly and briefly as follows.

The energy of the bombarding deuterons was established by setting up the desired magnetic field in the deflecting magnet.

The exact energy of the deuterons was measured precisely by exposing a photographic plate to observe elastically scattered deuterons from known target nuclei. (For E_d = 5.00 Mev, and

E_d = 5.74 Mev, V^{51} was used for this measurement; for E_d = 6.48 Mev O^{12} was used.)

After the elastic plate had been taken, successive survey plates were exposed; the deflecting magnet setting was left undisturbed, and adjustments were made only to the spectrograph magnetic field between runs.

The plates were developed and read, and the data were plotted. The experience of the Laboratory[3] has shown that the best ordinate for energy determination corresponds to a point 1/3 of the way up on the high-energy side of a peak. This ordinate seems to remain constant, regardless of target thickness or target exposure.

The calculations were then made, as discussed in Part III.

The bombarding energy was chosen subject to several governing factors. A good approximation for barrier height is

$$B = \frac{Z}{A^{1/3}} .$$

This shows that the Coulomb barrier is about 6.2 Mev for vanadium, so that it was desirable to have an energy of roughly that amount to minimize exposure time. We were limited at the upper end in bombarding energy by the fact that the spectrograph cannot be set up to analyze particles with momentum greater than that corresponding to a value of Hr of 479 kilogauss-centimeters, because the

E_g = 1.14 kev, γ_{32} was used for this measurement; for E_g = 6.18 kev β_{32} was used.)

After the plastic plate had been taken, successive scatter plates were exposed, the deflecting magnet reversing was fairly unsystematic, and adjustments were made only to the spectrograph current in fixed increments.

The plates were developed and read, and the data were plotted. The conservation of the momentum^2 has shown that the most probable for energy deficiency corresponds to a value $E/2$ of the way to the high-energy side of a peak. This relation seems to remain constant, regardless of target thickness or target composition.

The calculations were then made, as discussed in Part III.

The bombarding energy was chosen empirical to several powers of fourteen. A good approximation for intensity height is

$$I = \frac{E}{\gamma_{1/2}} .$$

This shows that the Compton intensity is about 6.3 per cent, so that it was desirable to have an energy of roughly that amount to minimize ecconomy time. We were limited at the upper end in bombarding energy by the fact that the accelerating current be not so large as to cause serious difficulties. Assume the

frequency of the present equipment is limited to 22.1 mcs. This momentum figure limits the energy of the protons to about 10.9 Mev. Since the Q-value of the $V^{51}(d,p)V^{52}$ reaction for the ground state is about 5.08 Mev, the maximum deuteron energy was limited to about 6.5 Mev for the ground state. The minimum effective operating voltage of the generator is about 4 Mev.

Between these two limits, we needed at least two bombarding energies widely enough separated to be of value in establishing the mass of the source of the groups. Thus, we arbitrarily chose to use E_d = 5.00 Mev and E_d = 5.74 Mev for the ground to 1.40-Mev levels and E_d = 5.74 and E_d = 6.48 Mev for the 1.40-Mev to 3.31-Mev levels.

With these bombarding energies, about a third of the proton groups fell in the region of Hr greater than 440, which is a region where the High Voltage group had operated very little previously. Inaccuracies were expected in this area because of slight field fringing at this high field setting. This effect appeared very slight on the basis of our results.

This region of high Hr presented another problem in that, here, both protons and deuterons are energetic enough to penetrate the 60-micron photographic emulsion and, thus, it would be impossible to distinguish protons from deuterons on the basis of track lengths. Therefore, the photographic plates were covered with two

layers of 1.5-mil aluminum foil, which was enough to stop deuterons and alpha-particles with this momentum, but it allowed the protons to pass through to the photographic emulsions.

In operating the equipment, our inexperience at first led us into several pitfalls. When any target exposure fails to yield useful information because of an avoidable mistake, the situation is disappointing, to say the least. More important is the fact that several man-hours and machine-hours are wasted. While it would be almost impossible to write completely detailed instructions for the operation of the equipment, the following "do's and don't's" could prove very useful to anyone knowing in general the operating procedure and yet having little operating experience:

1. Do not leave nuclear-track plates in the target room unless they are actually in the spectrograph. The high neutron flux in the room when the machine is operating causes "knock-on" proton tracks in the emulsion at random directions and makes accurate counting difficult or impossible.

2. Position the target so that none of the target frame is visible through the "C" chamber window. The positioning is critical, since the frame can yield a high background if it "sees" both the beam and the "C" chamber. Also, the target yield can be greatly reduced if the beam mark on the target is not well aligned with the "C" chamber entrance.

3. Remember that above an Hr of about 425 kilogauss-centimeters, it is not possible to distinguish between deuterons and protons by track lengths, when using 60-micron film without aluminum foil.

4. If aluminum foil is used, it must be as smooth as possible. Wrinkles tend to broaden the proton peaks and to randomize the angle of particle entrance into the emulsion. If banana oil is used to stick the foil, remember that the surface tension tends to "suck" the oil over the plate, ruining the area it covers. We found that attaching the foil to the plates with scotch-tape tabs was a preferable technique, as well as affording less danger to scratching the delicate emulsion during the foil removal; tabs on one edge act as a hinge after the other edge tabs were severed, thus allowing the foil to be lifted.

5. When loading plates, remember that the camera box can be isolated from the rest of the vacuum system and opened to atmosphere only when the plateholder is in the extreme in or extreme out position and the "C" chamber valve is closed. Opening the camera box to atmosphere at any other time will break the targets by allowing a sudden rush of air to enter the target chamber via the "C" chamber.

Part C. Target Preparation

The targets used in this experiment consisted of thin layers of pure vanadium evaporated onto thin Formvar backings which, in turn, were supported on target frames (shown in Figures 5 and 6).

The Formvar backing is prepared by dissolving about 1 gram of Formvar powder in 100 cc of ethylene dichloride. A drop of this solution placed on a smooth surface of distilled water forms a thin film which can be dipped upon the target frame. Film thicknesses of about a thousand Angstrom units can be made in this fasion. We found after considerable experience with the high temperatures developed in the evaporation system that six double layers of the film were the minimum amount which would stand up under the vanadium evaporation. The backings thus prepared are composed of carbon, oxygen, and a trace of nitrogen.

The evaporation system consists of a metal table upon which a bell jar is mounted on an annular rubber gasket. The table houses a liquid-air trap, an ion vacuum gage, a thermocouple vacuum gage, a control panel, a heating circuit, an orifice and plumbing system which leads to a mercury vapor pump, and a mechanical fore pump.

Four bronze rods screw vertically into the top of the table to form the support for the target frames, heating unit, and target material. Two of the rods are "wired" to supply the heat for the evaporation.

Figure 5

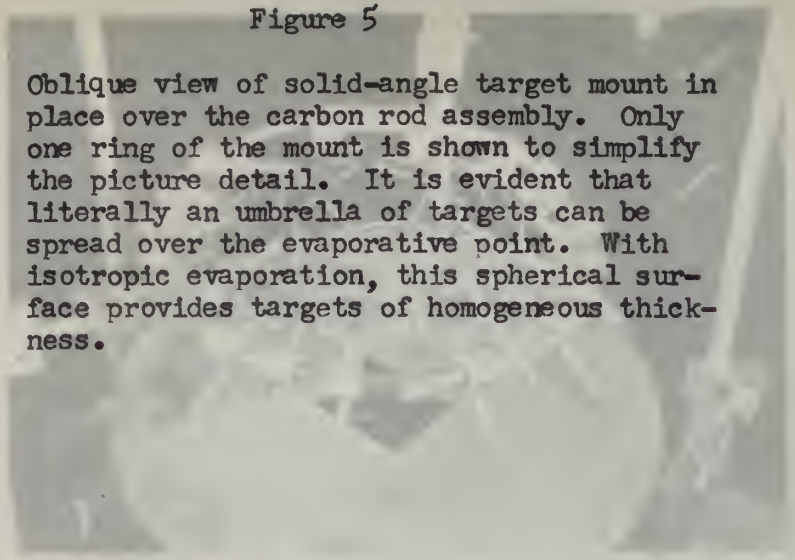

Oblique view of solid-angle target mount in place over the carbon rod assembly. Only one ring of the mount is shown to simplify the picture detail. It is evident that literally an umbrella of targets can be spread over the evaporative point. With isotropic evaporation, this spherical surface provides targets of homogeneous thickness.

Figure 6

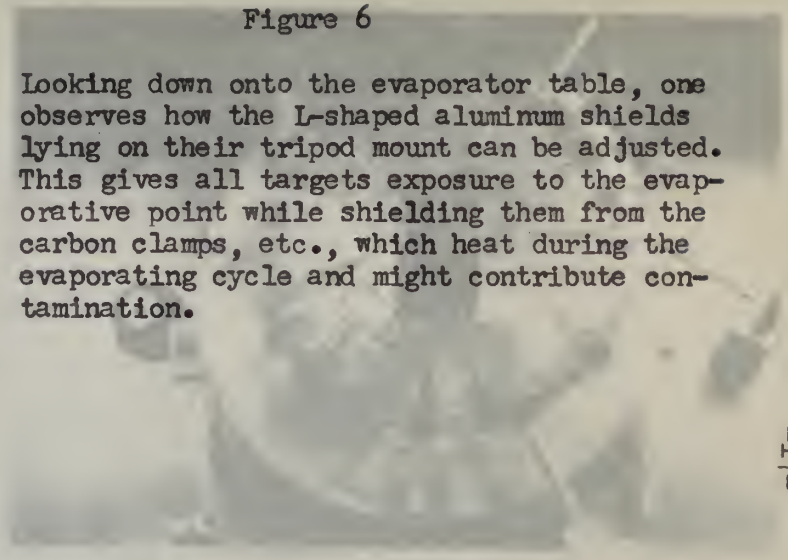

Looking down onto the evaporator table, one observes how the L-shaped aluminum shields lying on their tripod mount can be adjusted. This gives all targets exposure to the evaporative point while shielding them from the carbon clamps, etc., which heat during the evaporating cycle and might contribute contamination.

Figure 7

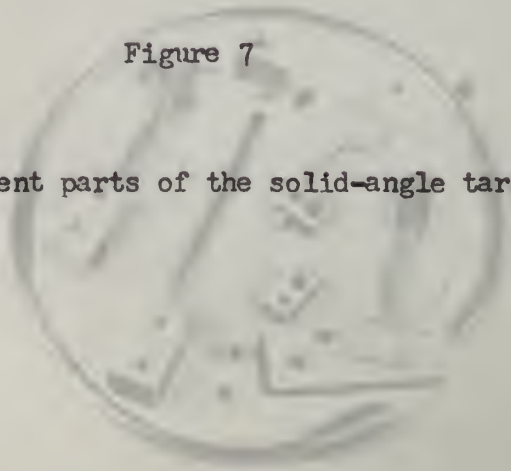

Component parts of the solid-angle target mount.

Figure 8

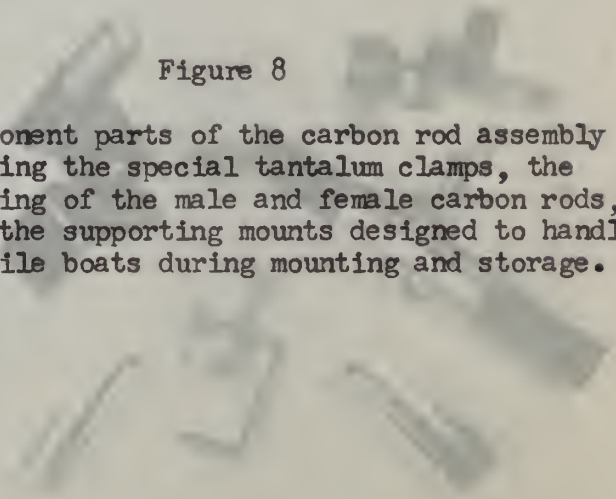

Component parts of the carbon rod assembly showing the special tantalum clamps, the shaping of the male and female carbon rods, and the supporting mounts designed to handle fragile boats during mounting and storage.

Figure 2

Optical view of solid-state target mount in place over the carbon rod assembly. Only one rim of the mount is shown to simplify the picture. It is evident that the entire mount may be lifted off as an assembly over the graphite electrodes with a technique similar to that used in changing a lens.

Figure 1

Component parts of the solid-state target mount.

Figure 8

Components of the carbon rod assembly.

Figure 7

Looking down onto the evaporated aluminum stripe, one of two parallel strips of carbon rod which are connected to the electrical feedthroughs. The slight curvature of the rods is to compensate for thermal expansion during heating.

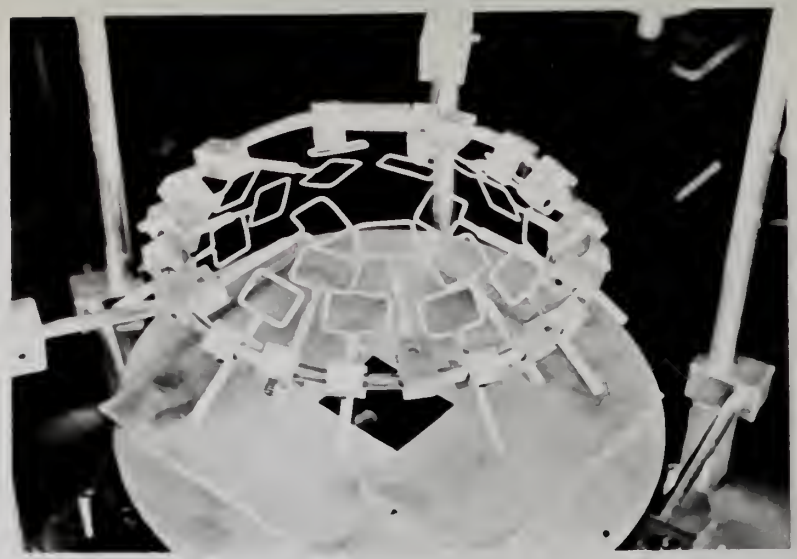

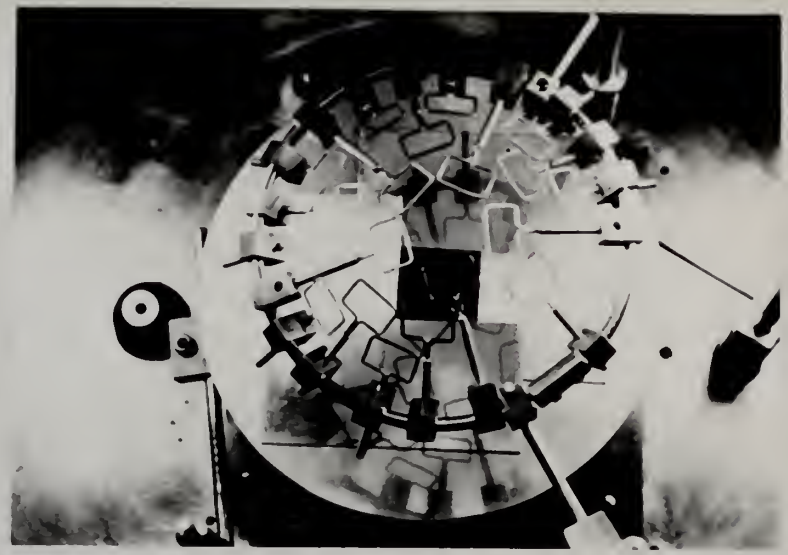

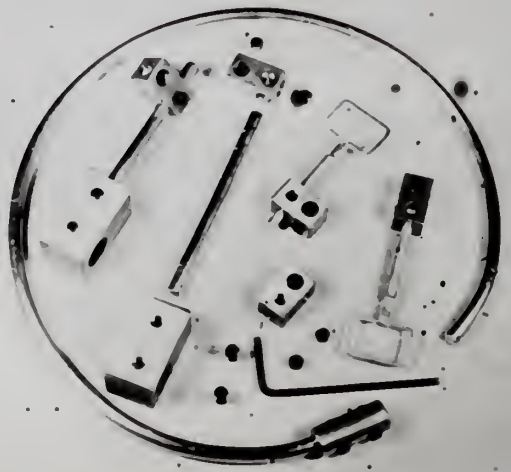

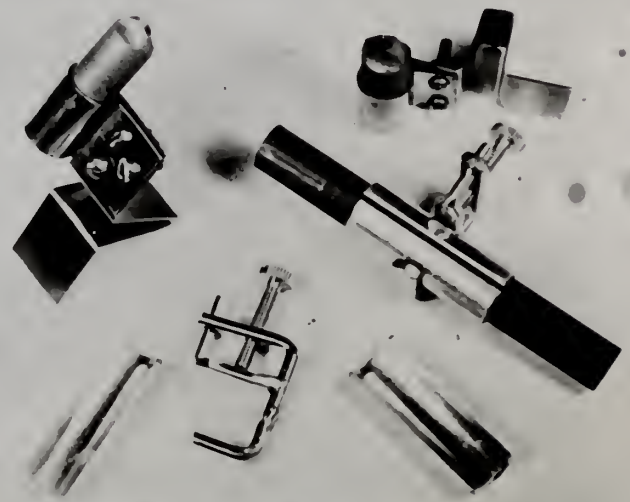

On the first attempts to evaporate the vanadium, we supported about eight target frames on horizontal rods clamped to the main vertical rods. A 1/2-inch carbon rod about 4" long was suspended between the wired rods by means of two tantalum "adapters" which held the carbon rod with good electrical contact. The adapters were held firm by stainless-steel clamps to the horizontal bronze rods. The carbon rod was "necked down" in the center and a hole was made in the top of this necked-down portion forming a "boat" in which to hold the vanadium pellets. The boat formed a high electrical resistance and, hence, concentrated the heat under the vanadium.

This method failed: If the heater current was brought up too quickly, the vanadium apparently vaporized locally and shot off "bullets" which broke the Formvar backings; if the heater current was brought up slowly enough, the vanadium melted uniformly, but it then made good electrical contact with the carbon. The resistance lowered at this point so that the heating was no longer localized at the vanadium.

Three steps were taken to improve the situation. First two brass rings were fashioned to be supported by the vertical rods and, in turn, support concentric rings of target frames (see Figures 5, 6, and 7). Care was taken during installation to center the assembly and to keep approximately equal radial distances from the evaporative

point. With this "solid angle" mount, we were able to form an umbrella of about twenty target frames and thereby increase our probability of realizing good targets on any single run; such an installation would also seem desirable for scarce or expensive materials. In addition, with such uniformity of intercepted solid angle, as well as nearly isotropic evaporation, we were able to produce nearly homogeneous groups of targets; this is a distinct advantage, since many targets are invariably needed to complete one's data. Another attractive feature of the mount is that the rings can be located at different radii, thus giving two distinct groups of targets (thick and thin) for a single run.

Second, an adjustable triped stand (see Figure 12) with a hole in the center was made which sat over the heating elements, and on this were placed two L-shaped pieces of aluminum. Thus, we were able to form an aperture over the spot where the vanadium was vaporized and to adjust the size of the aperture as desired by sliding the L-shaped pieces. This shielded the Formvar backings from the heat of the steel clamps, tantalum adapters, and carbon rod. It also reduced the hazard of target impurities from these sources.

Third, the idea of a carbon boat was abandoned, and, instead, two carbon rods, each about 2 inches long were suspended horizontally so as to "pinch" a vanadium pellet between the ends (see Figures 9,

Figure 9

Installation of fragile carbon boats without breakage is difficult. Here is demonstrated the advantage of using a supporting mount. Using this mount, we completely eliminated breakages during installation and storage.

Figure 10

Close-up of a vanadium pellet pinched between the male and female carbon rod. After the pellet is fused to the female rod, the top cover of the carbon cavity is ground away to give better isotropic evaporation. The male rod is then ground to nearly a filament point and held in compression against the fused pellet by the tantalum spring clamp.

Figure 11

Carbon rod assembly in place on the evaporator table showing the pinching action provided by the tantalum spring clamps.

Figure 12

The tripod shield mount is placed over the carbon rod assembly and adjusted so that all targets "see" the evaporative point.

Figure 9

Installation of fragile carbon posts without pressure is difficult. Here is demonstrated the advantage of using a swaddling mount. Using this mount, the fine carbon post is completely eliminated pressure during installation and storage.

Figure 10

Close-up of a vanadium pellet pinched between the male and female carbon rod. After the pellet is fixed to the female rod, the top cover of the carbon cavity is ground away to give better ground to nearly a flament point and held in compression against the fixed pellet by the tantalum spring clamp.

Figure 11

The turret shield mount is placed over the carbon rod assembly in Figure 10 and adjusted so that all tantalum "see" the evaporative point.

Carbon rod assembly in place on the evaporation support mounting bracket with the tantalum spring guide

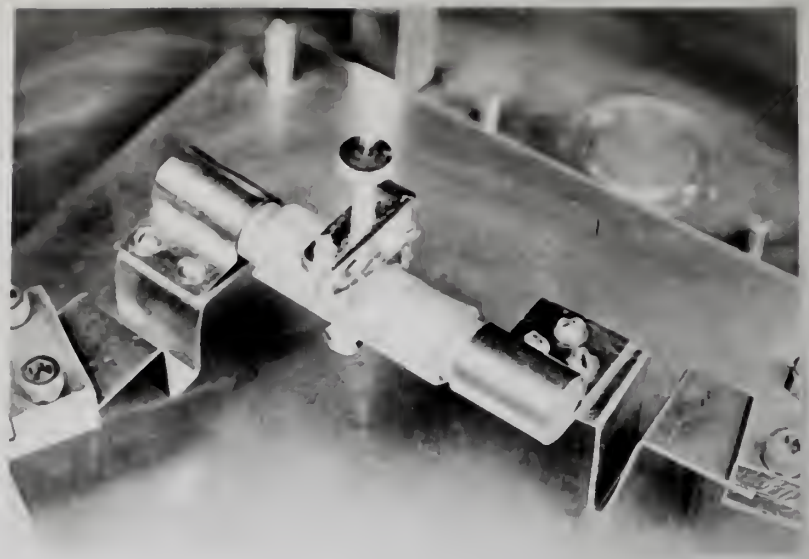

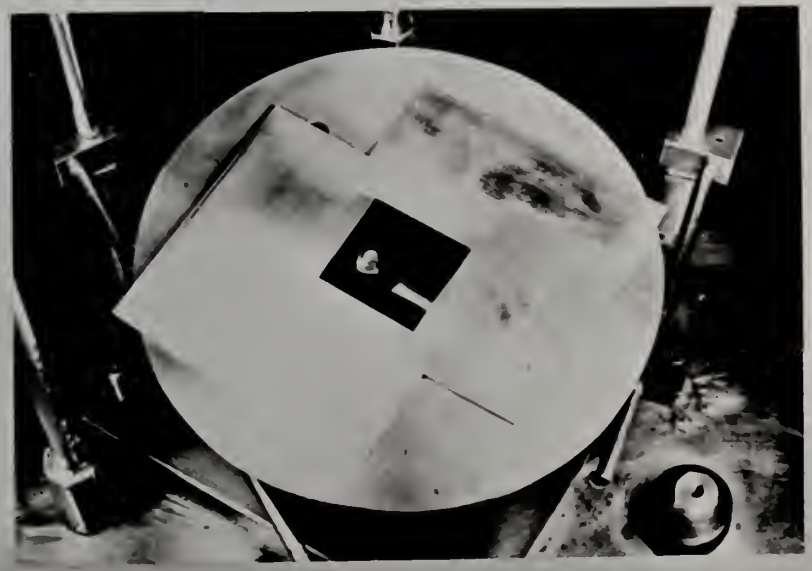

10, and 11). The adapters (Figures 9 and 11) were made so that they could exert longitudinal spring force on the carbon rods, as well as to tolerate torsion and expansion forces during the heating cycle.

In the end of one carbon rod, a small hole was ground to receive a vanadium pellet, and the other rod was sharpened for a point contact. It was found that the vanadium could then be fused to the female rod after which the top cover of the carbon cavity was ground away to afford better isotropic evaporation. The small rod was then ground to nearly a filament point, moved into contact position against the vanadium, and held under compression by the tantalum spring clamp.

Thus, the heat was concentrated on the vanadium, forming an "atomic spray gun" so to speak; the resistance did not change appreciably throughout the run, and it was possible to make very satisfactory targets with this arrangement.

After the vanadium was deposited, the targets were coated again with two double layers of Formvar. The resulting targets showed no sign of breakage under the beam after exposures of around 4000 microcoulombs.

10, and 11). The subplots (Figures 9 and 11) were made so that they could exert longitudinal gravity force on the carbon rods, as well as to tolerate traction and expansion forces during the heating cycle.

In the end of one carbon rod, a small hole was ground to receive a vacuum pellet, and the other rod was sharpened for a point contact. It was found that the vacuum could then be fixed to the female rod after which the top cover of the carbon cavity was ground away to afford better isotropic evaporation. The small rod was then ground to clearly a fifteen point, seven into constant position against the vacuum, and help under compression by the tantalum spring clamp.

Thus, the heat was concentrated on the vacuum, forming an "atomic sump pump" so to speak; the restrictions did not change appreciably throughout the run, and it was possible to make very satisfactory targets with this arrangement.

After the vacuum was deposited, the targets were cooled again with two double layers of Parafilm. The resulting targets showed no sign of breakage under the beam after exposures of around 1000 microcoulombs.

III. THEORY AND COMPUTATIONS

Part A. (d,p) Theory

The (d,p) reaction was considered anomalous for some time in that wave mechanics, which explained barrier penetration nicely, was unable to account for the occurrence of (d,p) reactions at deuteron energies low with respect to barrier height.

The Oppenheimer-Phillips explanation which appeared in 1935 explained the penetration at low energies by assuming that the deuteron "stretches out" radially with the proton part repelled by the Coulomb field and the neutron part continuing unopposed by the field until the neutron is absorbed and the proton is repelled. Thus, this stripping is more of a neutron-capture process than a real (d,p) nuclear reaction.

However, at higher energies, there is a greater chance that the whole deuteron is captured by the nucleus. Then the nucleus can re-emit a proton in a true (d,p) nuclear reaction.

Thus, the term (d,p) reaction really includes two different processes. The stripping reaction tends to emit protons in the forward direction, whereas the nuclear reaction is isotropic. Our experiment does not differentiate between the two because our measurements are made at 90 degrees to the incident beam.

III. Tensor and Spinor Fields

8. $(0,0)$ Tensors

The $(0,0)$ tensorfields were considered already for some time in their role as scalars, which constituted therefore practically also the only objects to account for the correspondence of $(0,0)$ tensorfields as physical variables has with respect to Lorentz-Inertia.

The Dirac-Pauli-Gordon wavefields which appeared in 1928 explained the elementarion at last accepted by nowadays that the physical electrons only partially with the proton part represented by the field until the neutron is adjusted and the proton is neglected. Then, data originally by mere of a correspondence problem in $(0,0)$ tensorfield.

Moreover, as higher energies, there is a greater chance that the whole neutron is captured by the nucleus. Then the nucleus can re-emit a proton in some $(0,0)$ neutron reaction.

Thus, the term $(0,0)$ wavefield mostly includes two different phenomena. The electron reaction helps to undo previous to the forward direction, whereas the neutron helps to transform. The exponential does not differentiate between the two because our measurements are made at 90 degrees to the incident beam.

Part B. Computations

Figure 13 shows the proton spectrum which resulted from the deuteron bombardment at 5.74 Mev. The plot was labeled by assigning letters alphabetically to each noticeable peak. If a peak seemed to have substructure, the subpeaks were numbered. Of these groups, only C seemed to be due to a known impurity. This seems to be the ground state of C^{14} from the $C^{13}(d,p)C^{14}$ reaction. The survey was not continued to the point where the first $C^{12}(d,p)C^{13}$ peak should appear. All the groups were then examined, as described below. Another such plot was obtained for the proton peaks down through F2 at deuteron energy of 5.00 Mev. A third such plot was obtained for the rest of the energy spectrum using a deuteron energy of 6.48 Mev.

In analyzing these data, it was noticed that the structure of the peaks did not reproduce itself exactly from one energy to another. These small changes made it impossible for us to specify completely the multiplet structure at O and P, for instance. Also, some of the smaller groups, such as E, did not reproduce clearly as peaks.

Therefore, we set up the following standards to apply to a group before we called it a probable level in V^{52}:

1. The peaks should have a maximum count of about 20 or more at each of the two deuteron energies so as to be something appreciably different from random background fluctuation.

Part 5. Conclusions

Figure 12 shows the various energies which resulted from the dominance hypothesized at 5.75 Mev. The plot was labeled by assigning level numbers objectively to each excitation peak. If a peak appeared in both reactions, the minimum were considered. Of course, only 0 seemed to be low in energy. This seems to be the ground state of C_{12} from the $C_{13}(t,\alpha)C_{12}$ reaction. The energy was not established by the point where the first $C_{13}(t,\alpha)C_{12}$ peak should appear. All the groups were taken seriously, as described below. Another weak peak was obtained for the reaction group through 12 at an excitation energy of 5.00 Mev. A third weak peak was obtained for the peak of the energy spectrum using a deuteron energy of 5.10 Mev.

In analyzing these data, it was noticed that the structure of the peaks did not reproduce itself exactly from one energy to another. There small changes made it impossible for us to specify completely the contingent resonance at 0 and 0, for instance. Also, some of the smaller groups, such as 3, did not reproduce clearly as peaks.

Therefore, we set up the following standards to apply to a group before we called it a probable level in Z^{22}.

1. The peaks should have a excitation energy of about 21 or more at each of the two deuteron energies so as to be reasonably separately different from random fluctuation.

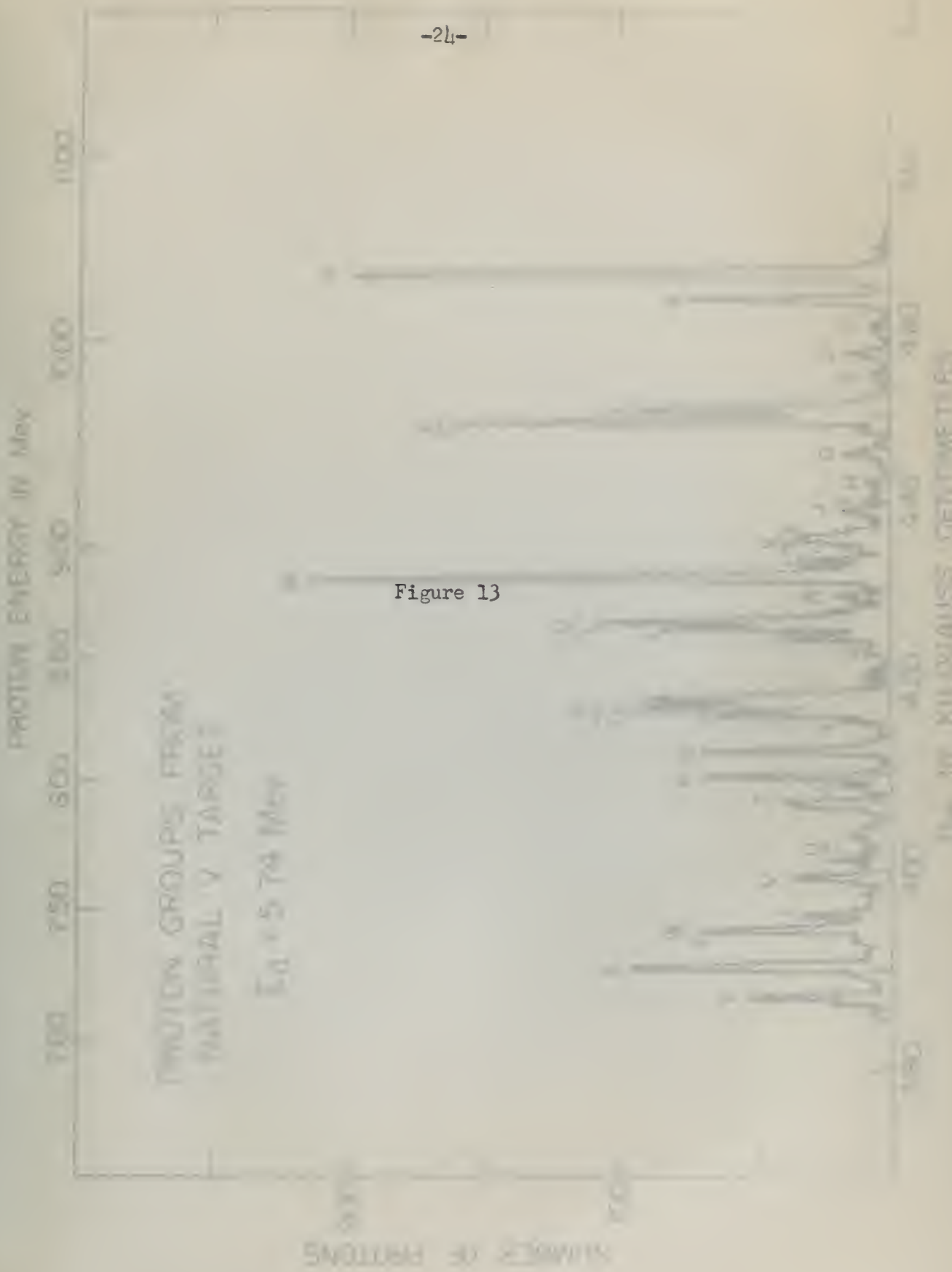
PROTON ENERGY IN Mev
700
750
800
850
900
950
1000
PROTON GROUPS FROM
NATURAL V TARGET
E1 = 5.74 Mev
IN KILOGAUSS CENTIMETERS
NUMBER OF PROTONS

Figure 13

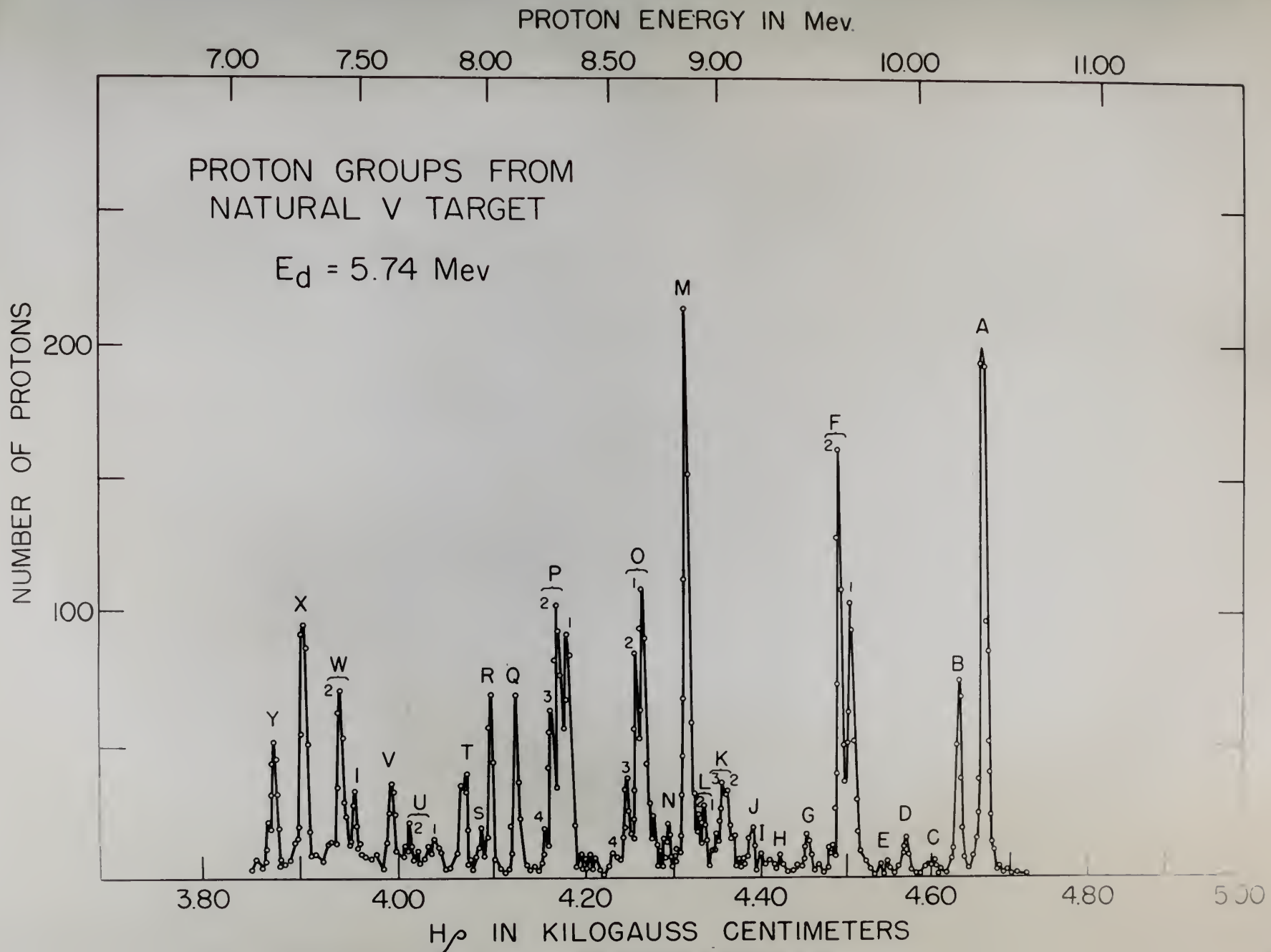
PROTON ENERGY IN Mev.
7.00
7.50
8.00
8.50
9.00
10.00
11.00
PROTON GROUPS FROM
NATURAL V TARGET
E_d = 5.74 Mev
NUMBER OF PROTONS
200
100
M
A
F
O
P
X
W
B
R
Q
Y
V
T
K
U
S
N
J
G
D
E
C
H
3.80
4.00
4.20
4.40
4.60
4.80
5.00
Hρ IN KILOGAUSS CENTIMETERS

2. The peaks should have a fairly clearly defined high-energy edge so that the 1/3 height could be well determined.

3. The Q-value should be determined to an agreement of 10 kilovolts or less from computations made from one or more exposures at each of at least two different energies. This requirement is apparent from the formula for Q-value:

$$Q = \frac{M_{res} + M_{out}}{M_{res}} E_0 - \frac{M_{res} - M_{in}}{M_{res}} E_{in} \text{ (for } 90^\circ \text{ emergence).}$$

Here for a given peak, both M_{res} and Q are unknown so an energy shift in E_{in} is necessary to give two equations to determine the two unknowns.

This third restriction is rather conservative in view of the probable error; however, it happened that all peaks which met the first two requirements also met the third.

A sample Q-value calculation is shown here as follows:

3. The peaks should have a fairly sharply defined high-energy edge so that the 1/2 height could be well determined.

3. The Q-value should be determined to an agreement of 10 kilovolts or less from computations made from not more experiments at least of at least two different energies. This requirement is expressed from the formula for Q-value:

$$Q = \frac{E_{rec} + E_{neut}}{E_{rec}} E_p - \frac{E_{rec} - E_p}{E_{rec}} \sin (\text{the two angles}).$$

Here for a given peak, both E_{neut} and Q are unknown as an energy shift in E_p is necessary to give two equations to determine the two unknowns.

This third restriction is rather conservative in view of the possible error; however, it happened that all peaks which met the first two requirements also met the third.

A sample Q-value calculation is shown here as follows:

Peak A, Plate 11N, Frequency 21.800 mcs, Index 11.100, E_d = 5.744 Mev (obtained from calculation of elastically scattered peak).

Index scale reading	11.100
1/3 height of peak	10.289
Δ	0.811
D_o	71.725 (calibrated)
Δ	-0.811
$2r$	70.914 centimeters
r =	35.457 cms

$$H = \frac{21.800 \text{ mcs}}{1.6546 \text{ mcs/kilogauss*}} = 13.1754 \text{ kilogauss.}$$

Hr = (13.1754)(35.457) = 467.159 kilogauss-centimeters.

E_{out}: 10.38786 (proton energy tables for Hr = 467 kg-cms)

704 = (0.159) x (Δ = 4428)**

E_o 10.39490

---

* from calibration.

** Δ is from tables of energy vs. Hr. Here linear interpolation is adequate

$$Q = \frac{M_{res} + M_{out}}{M_{res}} E_o - \frac{M_{res} - M_{in}}{M_{res}} E_{in} .$$

where:

$M_{res} = V^{52} = 51.96165$ (calculated as shown)

$M_{in} = {}_1H^2 = 2.014735$ (Li et al)

$M_{out} = {}_1H^1 = 1.008142$ (Li et al)

The computation for the mass of V^{52} is as follows:

$V^{51} + n = V^{52} + 7.305$ Mev (Bartholomew and Kinsey)

$d = n + p - 2.225$ (computed from data by Li et al)

$V^{52} = V^{51} + (d - p) - 5.080$ Mev

$= 50.96052^{4} + 1.006593 - 0.00546$

$V^{52} = 51.96165$

Therefore:

$$Q = 1.01940\ E_o - 0.96123\ E_{in}$$

$$\beta = \frac{S_{Pma} + S_{Pmb}}{S_{Pma}} \beta_p - \frac{S_{Pma} - S_{Pmb}}{S_{Pma}} \cos \omega$$

Where:

$S_{Pma} = S_{Pb}$ = 32.0805 (assigned as above)

$S_{Pm} = S_{Pc}$ = 5.0817E (IZ et al)

$S_{Pma} = S_{Pa}$ = 1.0021E (IZ et al)

The computation for the value of β_{PE} is as follows:

$\beta_{PI} + \beta$ = β_{PE} = 7.30E Hbr (Berthelsmeer and Kluwer)

β = 5.82E (computed from data by IZ et al)

β_{PI} = β_{PI} + (4 - 3) - 2.050 Hbr

= 10.9805β_p + 1.0051?3 = 0.30E6

β_{PE} = 11.9585

Therefore:

d = 7.0E60 β_p - 0.9583 β_{PE}

	10.59656
	-5.52131
Q =	5.075
Relativistic correction	.001
Q_{corr} =	5.076 Mev

The relativistic correction to the classical Q-value was determined according to the formula:

$$\Delta = (E_i)^2 \frac{M_{res}^2 - M_i^2}{1862\ M_{res}^3} + (E_o)^2 \frac{M_{res}^2 - M_o^2}{1862\ M_{res}^3} - \frac{M_i\ M_o}{931\ M_{res}^3} .$$

This positive correction was found to vary from about 0.8 kev for E_d = 5.74 Mev and E_p = 7 Mev to about 1.4 kev for E_d = 6.48 and E_p = 10 Mev, so that this correction was made by adding 1 kev to each classical Q-value obtained.

Part C. Survey of Impurities

In determining the Q-values, we obtained agreement to within 10 kev for the values obtained at the two different bombarding energies for each of the twenty proton groups. This agreement is better than could be expected considering the probable errors

	10.0808
	4.2131
ϕ =	5.875
Antiplatelets correction	.023
Cheese =	5.898 Rem

The multiplicative correction to the observed γ-value was determined according to the formula:

$$\Delta = (\Delta\gamma)^2 \frac{\gamma_{max}^2 - \gamma_1^2}{2\gamma_{max}\gamma_1} + (\Delta\gamma_1)^2 \frac{\gamma_{max}^2 - \gamma_1^2}{2\gamma_{max}\gamma_1} - \frac{\gamma_1 \gamma_2}{2\gamma_{max}^2}$$

This positive correction was found to vary from about 0.9 for the $\gamma_1 = 5.75$ Rem and $\gamma_2 = 7$ Rem to about 1.7 for the $\gamma_1 = 6.46$ and $\gamma_2 = 10$ Rem, so that this correction was made by adding 2 Rem to each observed γ-value obtained.

Test 5. Degree of Dependence

In determining the γ-values, we obtained agreement to within 10 Rem for the values obtained at the two different beamsetting energies for each of the energy proton groups. This agreement is better than would be expected considering the probable errors

assigned to the Q-values. However, if this ΔQ is assumed to be caused entirely by the wrong assignment of M_{res} in the equation for Q-determination, we can combine Q-equations for two different values of E_{in} to give:

$$\Delta Q = \left(\frac{M_{res} + M_o}{M_{res}}\right) \Delta E_o - \left(\frac{M_{res} - M_{in}}{M_{res}}\right) \Delta E_{in}$$

which, when solved for M_{res}, yields

$$M_{res} = \frac{M_o \, \Delta E_o + M_{in} \, \Delta E_{in}}{\Delta Q + (\Delta E_{in} - \Delta E_o)} .$$

Assuming $\Delta Q = \pm 10$ kev and the largest value of ΔE_o, we obtain an uncertainty in M_{res} of about 5 amu.

Of course, this means that mathematically the Q-values might have been caused by the (d,p) reaction with any nucleus of mass between 46 and 56.

The presence of any such impurity in an amount large enough to cause an appreciable proton yield does not seem possible, since the Formvar backings have been investigated extensively in the laboratory and shown to contribute only C, O, and faint N groups. The chemical analysis of the vanadium used in the evaporation is given by the Vanadium Corporation of America as:

assigned to the 1-value. However, if this is assumed to be caused entirely by the wrong assignment of Σ_{in} in the equation for C-determination, we can combine C-equations for the different values of Σ_{in} to give:

$$\Delta\Sigma = \left(\frac{\Sigma_{res} + \Sigma_{in}}{M_{res}}\right) \Delta C_0 - \left(\frac{\Sigma_{res} - M_{in}}{M_{res}}\right) \Delta\Sigma_{in}$$

which, when solved for Σ_{res}, yields

$$M_{res} = \frac{\Sigma_0 \Delta C_0 + \Sigma_{in} \Delta\Sigma_{in}}{\Delta\Sigma + (\Delta\Sigma_{in} - \Delta C_0)} .$$

Assuming $\Delta\Sigma = \pm$ 30 for and the largest value of ΔC_0, we obtain an uncertainty in M_{res} of about 5 mmb.

Of course, this means that particularly the 1-values might have been caused by the (d,p) reaction with some reactions between 1d and 2s.

The presence of any such impurity in an amount large enough to cause an inconsistency would have not been possible, since the Pasmany peaking have been investigated extensively in the laboratory and shown to contribute only C_0, D_0, and E_0 to a degree. The chemical analysis of the ammonium used in the preparation is given by the Standard Corporation of America as:

Vanadium Metal		(99.7 percent pure)
V	96.6 - 99.8	"
Si	.05	"
Fe	.05	"
Al	less than .05	"
N_2	less than .05	"
O_2	balance	

Here we need also note that vanadium is practically monoisotopic, consisting of

V^{51}	99.76 percent
V^{52}	.24 percent.

As an additional check on the impurities, a proton elastic survey was made of the actual target used. The survey extended from a mass of ∞ down through the carbon group. The plot of the survey is shown in Figure 14. An analysis of the peaks is given below: (for E_{in} = 6.52 Mev)

O^{16}	Balance	(99.7 percent pure)
C^{13}	less than .05	"
N^{14}	.03	"
N^{15}	less than .04	"
F^{19}	less than .05	"
Ne^{20}	.01 percent.	
Ne^{22}	10.78 percent	
Ne^{21}	89.19 percent	

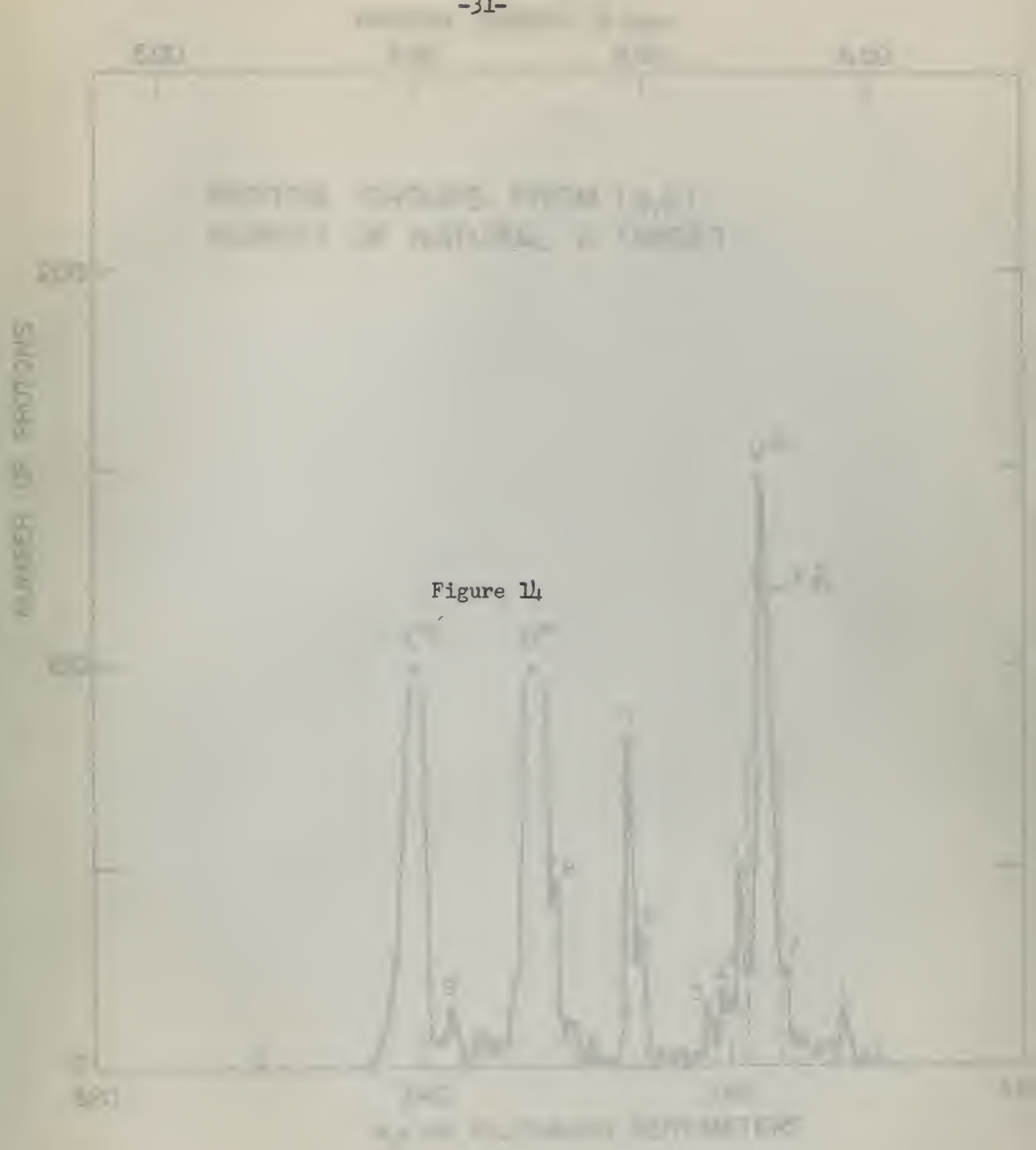

Figure 14

Figure 11

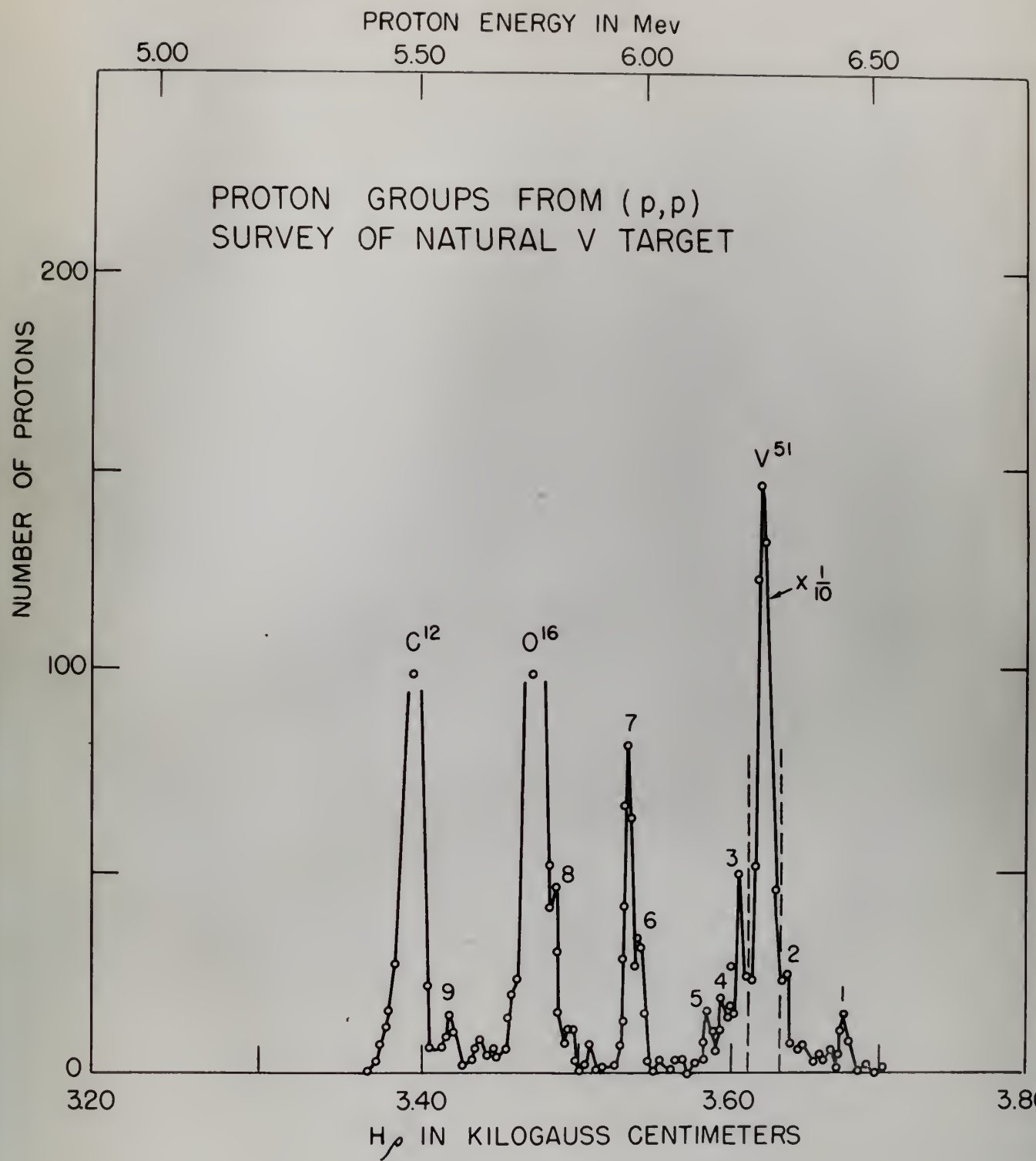
PROTON ENERGY IN Mev
5.00
5.50
6.00
6.50
PROTON GROUPS FROM (p,p)
SURVEY OF NATURAL V TARGET
NUMBER OF PROTONS
200
100
0
C12
O16
V51
X 1/10
7
8
6
9
3
4
5
2
1
3.20
3.40
3.60
3.80
Hρ IN KILOGAUSS CENTIMETERS

Designation	Maximum Proton Count	Apparent Source
1	15	Elastic scattering from M = 167
2	10	Elastic scattering from M = 62
3	30	Elastic scattering from M = 41
4	35	Elastic scattering from M = 34
5	15	Elastic scattering from M = 32
6	15	Elastic scattering from M = 23
7	80	V^{51*} (0.32) level
8	15	V^{51*} (0.48) level
9	40	Elastic scattering from M = 14.
V^{51}	1454	
O^{16}	Very large	
C^{12}	Very large	

Therefore, the elastic survey seems to show no trace of an impurity which could give rise to the peaks ascribed to V^{52}. However, it is fair to point out that the very impurities, which could theoretically cause the proton groups, are the ones which would be very difficult to detect in the large V^{51} peak.

Moreover, on the basis of the vanadium analysis and a consideration of the evaporation system, it is improbable that the groups tabulated later could be caused by any other reaction than $V^{51}(d,p)V^{52}$.

Configuration	Neutron Counts	Assigned Isomers
1	12	Kinetic scattering from 2 = 147
2	10	Elastic scattering from 2 = 42
3	20	Elastic scattering from 2 = 42
4	24	Elastic scattering from 2 = 34
5	25	Elastic scattering from 2 = 32
6	15	Elastic scattering from 2 = 23
7	80	h_{23} (0.32) level
8	15	h_{23} (0.42) level
9	50	Elastic scattering from 2 = 21
A_{23}	Very large	
C_{12}	Very large	
D_{12}	Very large	

Therefore, the elastic scatter seems to show no trace of an impurity which could give rise to the peaks associated to A_{23}. Moreover, it is fair to point out that the very impurities, which could theoretically cause the previous groups, are the ones which would be very difficult to detect in the large A_{23} peak.

Moreover, on the basis of the vacuolian analysis and a careful examination of the reconstruction system, it is improbable that the previous unexplained lines could be caused by any other reaction than $A_{23}(q,p)A_{23}$.

Part D. Probable Errors

The assignment of standard deviations or probable errors to the Q-values determined was not possible on a statistical basis, since the number of measurements was too small to permit a statistical treatment.

An uncertainty was arrived at by examining each step of the process by which a measurement is made in this laboratory. These sources of possible error[11] were the value of Hr for polonium alpha-particles, angle of incident beam with median plane of annular magnet, deviation of observation angle from 90 degrees, surface contamination of target, plate position, position of leading edge of group, stability of annular magnetic field, stability of deflecting magnetic field. An uncertainty was assigned at each step, and these sources of errors were compounded to give an over-all uncertainty of the quantity measured.

Elkind[6] made an analysis of this sort for the measurement of output energy and concluded that the fractional uncertainty is about 5.6:10,000.

Turner[12] made a statistical analysis for the measurement of input energy and concluded that the uncertainty in the measurement of input energy is about 0.1 percent. Although if E_{in} is measured from elastic scattering, the uncertainty should be the same as that for E_{out}.

Part D. Probable Errors

The assignment of standard deviations or probable errors to the Q-values determined was not possible on a statistical basis, since the number of measurements was too small to permit a statistical treatment.

In connection was carried on by examining each step of the process by which a measurement is made in this laboratory. There sources of possible error[11] were the value of π, for polarimeter alpha-particles, angle of incident beam with median plane of scattering segment, deviation of observation angle from 90 degrees, curvature of track, plane position, position of leading edge of group, stability of magnetic field, stability of deflecting magnetic field. An uncertainty was assigned at each step, and these sources of errors were considered to give an over-all uncertainty of the quantity measured.

Hafner[6] made an analysis of this sort for the measurement of output energy and concluded that the fractional uncertainty is about 5.5:10,000.

Terry[12] made a statistical analysis for the measurement of input energy and concluded that the uncertainty in the measurement of input energy is above 0.1 percent. Although if $\bar{E}_{in}$ is measured from elastic scattering, the uncertainty should be the same as that for E_{out}.

However,

$$Q = \left(\frac{M_{res} + M_o}{M_{res}}\right)E_o - \left(\frac{M_{res} - M_{in}}{M_{res}}\right)E_{in}$$

so that the uncertainty in Q is the square root of the sum of the squares of two terms, each of which is the product of an energy, its fractional uncertainty, and its mass ratio factor (near unity for V^{52}.)

For each Q-value, the highest value of E_o and E_{in} was chosen to give conservative results. This assumes that the leading edges of all peaks were equally well defined. The uncertainties all lay between 7.5 and 8.5 kev.

The value of 8 kev seems conservative, as far as reproducibility of data is concerned, since all of our Q-values fell within 5 kev of the average value.

The uncertainty of the level values was the square root of the sum of the squares of the ground-state uncertainty and the peak Q-value uncertainty. However, a smaller uncertainty in level separation can be arrived at whenever peak separations can be measured on the same plate.

IV. [illegible]

In closing remarks of the energy-level study, it is of course interesting to take note of previous work on the same subject.

Very little work has been done on the level nature of ^{62}Ni as compared with the large amount of information compiled for light nuclei; however, the ^{61}Ni(d,p)^{62}Ni reaction has been done several times previously.

The reaction was first done by Jentschke[2], who found levels at 2.47 and 3.70 Mev, using 3.3-Mv deuteron from a cyclotron. Later work on Q-values was done by Murray[3] and Murray Jarvis was compiled by Almqvist[4]. Since Almqvist's compilation of levels is the most nearly complete of these earlier (d,p) investigations, it is included for comparison. The agreement of our work with his was very satisfactory, but in view of the large uncertainties of his work, we have a possible agreement in each case.

The most nearly complete work on level nature was the published (d,p) by Bock of Pittsburgh and Kinsey[5], which along the results of Black's[6] investigation of these levels. However, the assignment of levels from gamma-ray energies is naturally confirmed by information, such as results from (d,p) work. These results are also tabulated for comparison.

Our levels confirm all of Bartholomew and Kinsey's levels within the uncertainties of the data. However, it is apparent that our values lie consistently lower than theirs.

Their work suggested that the 0.8 level was really two levels with a separation of 50 kev. There we have two well-separated groups at 0.780 and 0.834 Mev, a separation of 54 kev. Also, their gamma-ray peaks, F, J, and L, suggested possible levels which seem to correspond respectively with our 1.402, 2.307, and 2.848 levels. No peak was observed to correspond to their gamma-ray peak D.

The following table summarizes our results, along with those of Bartholomew and Kinsey, and those of Abramov:

TABLE I

Group	Relative Intensity for E_d = 5.7h	Present Work: Q-Value in Mev	Present Work: Level Values in Mev	Previous Results: Kinsey	Previous Results: Abramov
A	0.93	5.072 ± 0.008	0		
B	0.36	4.941 ± 0.008	0.131 ± 0.011	0.15 ± 0.01	
D	0.07	4.654 ± 0.008	0.418 ± 0.011	0.44 ± 0.01	
F_1	0.50	4.292 ± 0.008	0.780 ± 0.011	0.80 ± 0.01	0.72 ± 0.08
F_2	0.75	4.238 ± 0.008	0.834 ± 0.011		
K_2	0.21	3.670 ± 0.008	1.402 ± 0.011		1.31 ± 0.08
L	0.13	3.597 ± 0.008	1.475 ± 0.011		
M	1.00	3.527 ± 0.008	1.545 ± 0.011	1.56 ± 0.01	1.65 ± 0.08
O_1	0.50	3.319 ± 0.008	1.753 ± 0.011		
O_2	0.18	3.287 ± 0.008	1.785 ± 0.011	1.79 ± 0.01	
P_1	0.43	2.984 ± 0.008	2.088 ± 0.011	2.10 ± 0.01	2.04 ± 0.08
Q	0.40	2.765 ± 0.008	2.307 ± 0.011		

Variable	Results
0.0 ± 0.0	0.0 ± 0.0

	Control group	Experimental group	Statistical significance (p < 0.05)	Effect size
n	0.0 ± 0.0	0.0 ± 0.0	0.0	0.0
t_{df}	0.0 ± 0.0	0.0 ± 0.0	0.0	0.0
F_{df}	0.0 ± 0.0	0.0 ± 0.0	0.0	0.0
χ^2_{df}	0.0 ± 0.0	0.0 ± 0.0	0.0	0.0
r_{df}	0.0 ± 0.0	0.0 ± 0.0	0.0	0.0
p_{df}	0.0 ± 0.0	0.0 ± 0.0	0.0	0.0

B I B L I O G R A P H Y

1. Abramov, A. Y., Akad Nauk. USSR Doklady 73 (No. 5) 923 (1950)
2. Bartholomew, G. A. and B. B. Kinsey, Phys. Rev. 89, 386 (1953)
3. Buechner, Strait, Sperduto and Malm, Phys. Rev. 76, 1543 (1949)
4. Collins, Mier, and Johnson, Phys. Rev. 86, 408 (1952)
5. Davidson, W. L., Phys. Rev. 56, 1061 (1939)
6. Elkind, M. M., Ph. D. Thesis, M. I. T., May 1953
7. Enge, H. A., Rev. Sci. Instr. 23, 599 (1952)
8. Harvey, J. A., Phys. Rev. 81, 353 (1951)
9. Li, Whaling, Fowler, and Lauritsen, Phys. Rev. 83, 512 (1951)
10. Strait, E. N., Jr., Ph. D. Thesis, M. I. T., May 1948
11. Strait, Van Patter, Buechner, and Sperduto, Phys. Rev. 81, 747 (1951)
12. Turner, E. F., Jr., M. S. Thesis, M. I. T., September 1952

BIBLIOGRAPHY

1. Ashmore, A. T., Ahmd Disc. USTH Technol 73 (No. 5) 653 (1950)

2. Berglund, O. R. and E. R. Kaul, Chem. Engr. Prog. Symp. Ser. 59, 244 (1963)

3. Bergman, Chemistry, Chemistry and Life, Chem. Eng. Ser. 76, 1263 (1959)

4. Coulson, Richardson, and Backhurst, Chem. Eng. Vol. 6, 6th (1996)

5. Treybal, R. E., Chem. Eng. Vol. 56, 1963 (1949)

6. Kolbel, H. H., Jr. D. Chemie, W. I. T., Sep 1963

7. Thom, W. A., Proc. Ind. Instr. 53, 596 (1962)

8. Perry, J. H., Chem. Eng. Vol. 61, 263 (1963)

9. W. Walking, Technic, and Instrument, Chem. Eng. 63, 532 (1953)

10. Church, I. H., Jr., Sc. D. Chemie, W. I. T., Sep 1956

11. Hewitt, Van Tuyker, Instrument, and Systems, Chem. Eng. 63, 967 (1952)

12. Thomas, R. I., Jr., M. S. Chemie, M. I. T., September 1952